Optical properties of metallic sodium tungsten bronzes: Analysis of free- and bound-electron contributions

P. Camagni and A. Manara
Physics Division, J.R.C. Euratom, Ispra, Italy

G. Campagnoli, A. Gustinetti, and A. Stella
Istituto di Fisica dell'Università di Pavia and Gruppo Nazionale di Struttura della Materia del Consiglio Nazionale delle Ricerche, Unità di Pavia, Italy

(Received 6 May 1976)

Monitoring of the optical response of Na_xWO_3 of varying stoichiometric ratio was performed by means of ellipsometry (from ~ 0.3 to 5.2 eV) and electromodulated reflectance (from 1.3 to 3 eV). The spectra of the real and imaginary part of the dielectric function were used to separate free-electron and bound-electron components, providing direct evaluation of the carrier-density to effective-mass ratio as well as of the carriers relaxation rate. Electroreflectance spectra gave evidence of major modulation structure associated with the plasma edge; this was explicitly analyzed with the help of ellipsometric data and shown to be compatible with the existence of a modulated transition layer at the metal-electrolyte interface. A smaller structure in the electroreflectance spectra, occurring at lower energies, was explained in terms of a band-population effect. Its discussion, together with the knowledge of free-electron parameters, allows a certain characterization of the conduction states, based on current theoretical band schemes for similar compounds.

I. INTRODUCTION

The electronic structure of alkali-tungsten bronzes has been repeatedly investigated in recent years, mostly via their optical[1-4] or electrical[5-9] properties. Optical measurements have provided a variety of information on qualitative aspects, in particular (a) a picture of interband transitions in fair agreement with a general scheme common to many ABO_3 dielectric perovskites or related structures such as the bronzes[10-12] and (b) the existence of an important free-carrier contribution, evidenced by the characteristic dip of reflectivity and its dependence on stoichiometry.[1,2,4]

Optical studies have not been able so far to provide quantitative monitoring of interband and intraband contributions, in the region where the two coexist. This leaves open, among other aspects, the determination of basic parameters of the conduction electrons. A full comparison with corresponding data from electric transport experiments is therefore not possible.

Starting from the above considerations, we have undertaken a systematic study of the optical response of a series of Na_xWO_3 compounds of different stoichiometries in the region between ~0.30 eV and the first interband transition, by means of distinct but complementary reflection techniques. The first technique is ellipsometry, by which the absolute spectra of the complex dielectric function were obtained in the region of interest. The second technique is electroreflectance, by means of which finer structure in the region of the reflectivity minimum was studied.

II. MEASUREMENTS OF THE OPTICAL CONSTANTS

The ellipsometric measurements for the determination of ϵ_1 and ϵ_2 (real and imaginary part of the complex dielectric function) were taken with a reflection arrangement described in another paper.[13] The experiments were based on known methods,[14,15] in which full determination of the ellipticity of reflected light is achieved by measuring four distinct intensities, which are reflected by the sample along four different azimuths. In this way the ellipsometric quantities of interest (i.e., amplitude ratio and relative phase of the principal components of reflected light) were measured. The optical constants were then derived through standard relationships of physical optics.[16] In order to minimize the errors measurements were systematically performed in conditions of principal incidence.[14,15]

For the analysis of polarized light, two sets of polarizers were used: (a) a pair of high-quality Glan-Taylor prisms in calcite, for the region between 0.235 and 2.4 μm; (b) a pair of Glan-Thompson prisms, cut to design from single-crystal rutile (TiO_2) for the region between 2.4 and 5 μm.[17] The depolarized transmission residue of these pairs was of the order of 10^{-5} and 10^{-4}, respectively, at all wavelengths.

Illumination of the ellipsometer came from a two-prism monochromator; the light sources were tungsten filament lamps with appropriate windows.

To avoid problems due to parasitic light, continuous sources were replaced below ~0.33 μm by a set of spectroscopic line sources, extending

the observations to a certain number of fixed wavelengths down to the quoted limit of the calcite prisms.

The surface of the samples was prepared to optical finish by means of mechanical polish, followed by ultrasonic cleaning and by chemical etching in a deoxidizing solution. The sample was transferred for the experiments to an argon-flushed optical cell, mounted at the center of the ellipsometric goniometer. The cell had a cylindrical window made in special strain-free silica glass, transmitting up to ~3.3 μm. Use of this cell prevents progressive oxidation, which is harmful to measurements of the optical constants in the visible and uv regions.

After completing the observations in the range compatible with the cell, the sample was repositioned in open air and measurements above 3 μm were continued. In this region, the effect of thin oxidation layers is practically negligible.

The accuracy of the present experiments was mainly limited by statistical errors of photometric origin. The overall errors are thus 4%–6% for values of ϵ_1 and ϵ_2 of the order of 0.5 or higher; they rise rapidly above 10% for values of the optical constants around 0.1. This is the case in a certain interval near the reflectivity dip; the corresponding data have not been considered in quantitative analysis, even when their qualitative behavior appeared to be regular.

A. Results and analysis

Figures 1–3 give the measured spectra of the optical constants, for Na_xWO_3 of different stoichiometric ratios ($x = 0.52$, 0.72, 0.85). Each spectrum is divided in two sections, so as to provide a magnified view of the visible and uv range. The optical response is seen to exhibit three distinct regions of behavior in each compound:

(i) The region between the ir limit and the onset of the visible range, in which the absolute values of ϵ_1 and ϵ_2 undergo a rapid, monotonic decrease over at least two orders of magnitude, without noticeable structure. Such a behavior agrees with the indications of earlier reflectivity studies and gives further evidence of the role of intraband transitions.[2,4,10]

(ii) An intermediate region, in which ϵ_1 crosses the zero line, merging continuously into the tail of a structure that develops at higher energies. Correspondingly, ϵ_2 continues to decrease and reaches a minimum, giving a neat separation between the monotonic range and the structure in the near uv. The value of ϵ_2 in this minimum agrees satisfactorily with the value obtained by Kramers-Kronig analysis of reflectivity data in a similar

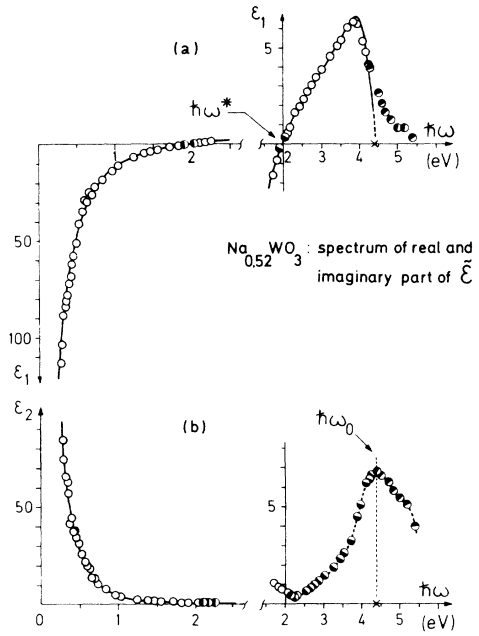

FIG. 1. Room temperature optical response of $Na_{0.52}WO_3$. (a) Spectrum of ϵ_1; (b) spectrum of ϵ_2. Open circles represent data points used in best-fit analysis. Solid lines are best-fit curves according to parameters in Table I. Hatched lines are graphical interpolations. $\hbar\omega^* = 1.95$ eV; $\hbar\omega_0 = 4.40$ eV.

compound.[4] The energy of zero crossing in the ϵ_1 spectrum, $\hbar\omega^*$, is clearly defined only in the case of $x = 0.52$; in the other compounds it is somewhat masked by a weak, unexplained anomaly,[18] but it can be determined with the help of graphical

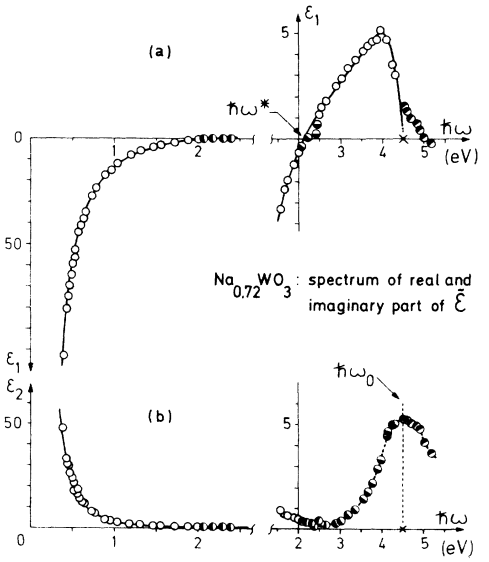

FIG. 2. Same as Fig. 1, for $Na_{0.72}WO_3$. $\hbar\omega^* = 2.12$ eV; $\hbar\omega_0 = 4.55$ eV.

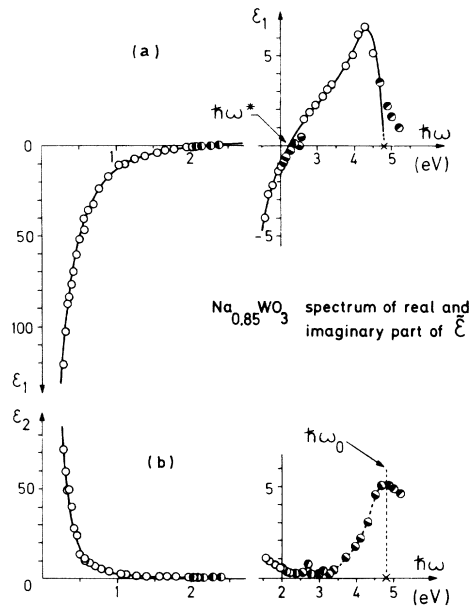

FIG. 3. Same as previous figures, for $Na_{0.85}WO_3$. $\hbar\omega^* = 2.23$ eV; $\hbar\omega_0 = 4.80$ eV.

extrapolation from adjacent regions.

(iii) The near uv region, characterized by definite structure of both spectra. In the case of ϵ_2, this structure is represented by one major peak, with hints of unresolved components on the high-energy side. The apparent peak energies $\hbar\omega_0$, also shown in the figures, are in increasing progression with respect to x, closely similar to that of the $\hbar\omega^*$'s.

The main feature of ϵ_1 is a relatively sharp inversion, followed by a region of negative slope, which correlates with the position of the ϵ_2 peak and shifts accordingly. This spectrum is also modified by minor structure on the high-energy side and by progressive lifting of the background in the extreme uv. The latter might be due to the tail of high-energy structures, already detected in reflectivity work.[4]

Though the frequency and the accuracy of our data do not warrant a closer examination of spectral details, it seems reasonable to interpret the general behavior of ϵ_1 and ϵ_2 in the near uv as the "dispersion" and "absorption" counterparts of the optical response associated with one dominant mechanism. Such mechanism should be the first interband transition for which a plausible assignment, in the case of dielectric perovskites, would be X_5, (valence) $\rightarrow X_3$ (conduction).[12(a)] In the metallic case, this interpretation is no longer acceptable, since the X_3 minimum is occupied. As an alternative, various transitions from the valence set, or the lower conduction manifold, to higher conduction states could be taken into consideration, as proposed in Ref. 4. In any case, transitions across the Fermi level would leave unexplained the observed dependence of ω_0 with stoichiometry.

Lacking the elements for deeper discussion, we shall not argue about the origin of the prominent uv structure, and limit ourselves to analyze its spectral shape on purely formal grounds.

The present results were subjected to a systematic analysis, in order to test a specific model of the optical response. Care was taken especially to work out the low-energy region of the spectra, so as to obtain the relevant parameters of the free-electron gas. This approach is justified by two outstanding features of the quoted region, i.e., smooth energy dependence, suggesting a major role of intraband absorption, with little perturbation from bound electrons up to at least 2 eV and large overall variations (two orders of magnitude) in the optical constants. This allows for a consistent application of best-fit procedures.

The spectrum $\epsilon_2(\omega)$ was analyzed first on account of its evident separation between free-electron and bound-electron contributions. Accordingly, the fitting was carried out with an idealized Drude model of the type

$$\epsilon_2(\omega) = 4\pi e^2 (N/m)[\gamma/\omega(\omega^2+\gamma^2)] \tag{1}$$

using only data points below the apparent plasma energy. The ratio N/m (conduction-electron density to electronic mass) and the relaxation rate γ were in this case the adjustable parameters. An iterated least-squares procedure was employed in this, as well as in subsequent fittings.

For the analysis of $\epsilon_1(\omega)$, the model function was more comprehensive, so as to take into account the free-electron polarizability as well as a term of bound-electron polarizability, describing the effect of the first interband transition. The latter was represented by a damped harmonic oscillator, whose resonant frequency ω_0 was made to coincide with the observed peak position of the ϵ_2 structure.

Accordingly, the total dielectric function was expressed with four independent parameters, as

$$\epsilon_1(\omega) = \epsilon_\infty - 4\pi e^2 \frac{N}{m} \frac{1}{\omega^2+\gamma^2} + \frac{A(\omega_0^2-\omega^2)}{(\omega_0^2-\omega^2)^2+\omega^2\Gamma^2}, \tag{2}$$

where N/m has the same meaning as before, A and Γ are the amplitude factor and the damping constant of the oscillator and ϵ_∞ includes a possible residue coming from higher-lying transitions, which are known to occur in the region above 8 eV.[4]

At this stage the relaxation rate γ for free electrons was no longer defined as a running param-

eter, on account of its negligible influence on the quality of fittings. For the sake of consistency, its value was worked out by the program as a specific function of the other parameters; this is obtained from expression (2), imposing the empirical constraint $\epsilon_1(\omega^*) = 0$ and using the observed energies of zero crossing.

The above analysis was applied to both spectra, for the three stoichiometries. The final results are summarized in Table I, listing the best-fit values of the various parameters entering the model functions (1) and (2). A graphical appreciation of these results is readily made observing the best fit curves of Figs. 1–3.

The fitting of dispersion spectra was the more satisfactory. In fact, the root-mean-square deviation of the theoretical curves with respect to the experimental data was in every case of the order of 7% or lower, whereas the corresponding deviation in the case of ϵ_2 spectra was $\gtrsim 10\%$. We ascribe this larger uncertainty to the restricted spectral range considered in the treatment of ϵ_2, hence to the large proportion of points with values below unity, for which the experimental error is probably greater than the statistical estimate. In the case of ϵ_1, only a few points on the extreme uv side of the direct transition were discarded, owing to the existence of residual dispersion which could not be included into the present model. Though the final fits are not expected to give an optimal representation of the uv structure as such, they certainly provide sufficient refinement in the intermediate region to insure that the free-electron range is accurately reproduced.

In view of the above remarks, it is not surprising that the values of N/m, derived from the two independent sets of data, differ systematically by (10–20)%, for any given stoichiometry.

III. ELECTROREFLECTANCE

The first observation of electroreflectance in metals by means of the electrolytic cell is due to Feinlab.[19] The attribution of the effect observed to the modulation of the optical constants of the metal, the electrolyte, or a combination of both, was discussed by several authors. In some cases the spectra have been satisfactorily fitted using specific models, involving different physical mechanisms, some of which are based on the presence of a third phase between the metal and the electrolyte.[3,19-22]

Our measurements were made in the energy range 1.3–3 eV, using a standard electrolytic cell in a two-electrode configuration; the sample was working as an electrode (light impinging upon it at near-normal incidence) and a Pt plate was the other electrode. The electrolytic solution was 0.1*N* KCl in water. Different dc polarization voltages, in the range −0.5–+0.5 V were chosen, whereas the superimposed ac component was given peak-to-peak values up to a maximum of 1 V. The frequency of the modulating field was ≤ 200 Hz. It is important to observe that, for the quoted values of the dc bias, the particular value chosen for the other two parameters (frequency and ac voltage) affected the absolute value of $\Delta R/R$ at any given λ, but not the presence or line shape of actual structures.

The samples were those used in the ellipsometric observations and were subjected to the treatments specified in Sec. II.

A. Results and analysis

In Fig. 4 $\Delta R/R$ spectra are reported for the three stoichiometries under examination. At these values of x the behavior is known to be metallic.

TABLE I. Parameters of free and bound electrons in $Na_x WO_3$, according to best fit of intraband and interband contributions to ϵ_1 spectra. Figures in parentheses are taken from the analysis of ϵ_2 spectra (intraband only). Amplitude and damping rate of the uv oscillator are expressed in terms of the resonance frequency ω_0. The entity of ϵ_∞ is probably not a faithful determination of the high-frequency dielectric residue, as it may contain additively an unknown correction of the ordinate scale (of the order of 0.1).

Stoichiometric ratio, x	Free-electron parameters N/m (10^{49} cm^{-3} g^{-1})	γ (10^{14} sec^{-1})	ϵ_∞	Harmonic oscillator parameters A (units of ω_0^2)	Γ (units of ω_0)
0.52	1.34		1.47	2.33	0.21
	(1.11)	(0.97)			
0.72	1.37		1.45	1.83	0.22
	(1.26)	(0.49)			
0.85	1.48		1.03	2.08	0.18
	(1.24)	(0.37)			

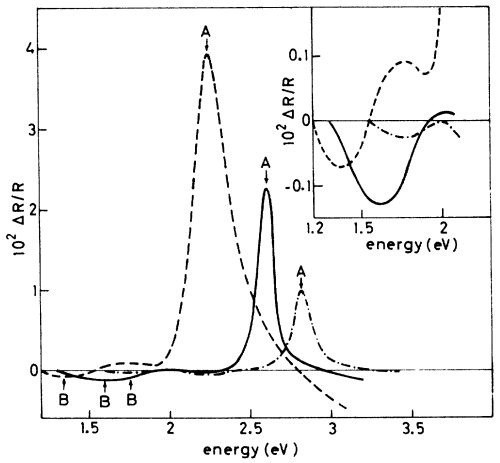

FIG. 4. Normal-incidence electroreflectance spectra of Na_xWO_3 samples with stoichiometries: $x=0.52$ (---); $x=0.72$ (——); $x=0.85$ (— • — •). The insert shows a magnified view of structure B. External voltage applied between sample and Pt electrode. Operating conditions: dc bias is 0 V; peak-to-peak ac voltage ≤ 1 V; frequency is 35 Hz.

In all of the samples examined two typical structures show up:

(i) A strong peak (quoted as structure A) whose position is correlated to the reflectivity minimum and shifts accordingly towards higher energies with increasing x. Peak positions are actually 0.1–0.2 eV higher than those of the above quoted minimum.

(ii) A weaker structure of opposite sign (structure B) at lower energies, whose position also increases with stoichiometry.

Several attempts have been made to fit the experimental profile of the A structure (namely line shape and energy position) with theoretical expressions derived from different models. A satisfactory fitting was obtained using a particular model, due to McIntyre and Aspnes and based on a three-phase system.[22] This treatment, in its original form, rests on the following assumptions:
(a) The existence of a transition layer between the metal and the electrolyte, having a thickness $d \ll \lambda$ and a dielectric function $\hat{\epsilon}_{TL}$: (b) a complex dielectric function of the metal given by a combination of intraband and interband components $\hat{\epsilon}_M = \hat{\epsilon}_{Mf} + \hat{\epsilon}_{Mb} + \hat{\epsilon}_{M\infty}$; (c) only the free-electron component $\hat{\epsilon}_{Mf}$ is modulated by the electric field.

As the electric field is modulated between E and $E+\Delta E$, the reflection coefficient of the three-phase structure is modulated between R_E and $R_{E+\Delta E}$ with an observed modulation of the fractional reflectivity:

$$\frac{\Delta R}{R} = \frac{R_{E+\Delta E} - R_E}{R_E} \simeq \frac{8\pi n_D d}{\lambda} \operatorname{Im} \frac{\langle \hat{\epsilon}^* \rangle_{E+\Delta E} - \langle \hat{\epsilon}^* \rangle_E}{n_D^2 - \hat{\epsilon}_M}, \tag{3}$$

where n_D is the refractive index of the electrolyte and

$$\langle \hat{\epsilon}^* \rangle = \frac{1}{d} \int_{-d}^{0} [\hat{\epsilon}_{TL}(z) - \hat{\epsilon}_M] dz \tag{4}$$

is the average distortion of the dielectric function of the layer with respect to that of the metal.

Supposing that the transition layer is a perturbed surface region of the metal and recalling condition (c) the modulation of $\langle \hat{\epsilon}^* \rangle$ can be expressed in terms of the fractional change of carrier density $\Delta N/N$:

$$\Delta \langle \hat{\epsilon} \rangle \equiv \langle \hat{\epsilon}^* \rangle_{E+\Delta E} - \langle \hat{\epsilon}^* \rangle_E = \frac{\Delta N}{N} \frac{\hat{\epsilon}_{Mf}}{d}. \tag{5}$$

The combination of Eqs. (3) and (5) yields

$$\frac{\Delta R}{R} = \frac{8\pi n_D}{\lambda} \frac{\Delta N}{N} \operatorname{Im} \frac{\hat{\epsilon}_{Mf}}{n_D^2 - \hat{\epsilon}_M}. \tag{6}$$

A comparison was made between experimental electroreflectance spectra and the theoretical curves derived from Eq. (6), using the experimental values of $\hat{\epsilon}_M(\omega)$ given in Figs. 1–3 and values of $\hat{\epsilon}_{Mf}$ as calculated from Eqs. (1) and (2) with the help of the pertinent parameters listed in Table I. Figure 5 illustrates this comparison for the case $x=0.52$ and $x=0.85$. With this method we found that the peak heights were fitted if $(\Delta N/N)d \simeq 0.85 \times 10^{-8}$, 0.5×10^{-8}, 0.11×10^{-8}, respectively, in order of increasing stoichiometry. The line shape of the A spectrum was satisfactorily fitted in all cases, whereas the energy position required small adjustments between 0.09 and 0.03 eV.

While this model accounts for the modulation spectrum near the reflectivity minimum, it does not predict any structure at lower energies, in contrast with the experimental evidence of structure B. Typical features of this component are (a) its energy position is an increasing function of x and (b) at a given stoichiometry, there is a shift of ~0.1 eV towards higher energies if the polarization voltage is varied from −0.5 to +0.5 V. A detailed discussion of the B structure will be given in Sec. IV.

IV. DISCUSSION

We comment first on the parameters of the free-electron gas, in order to have some characterization of the conduction states.

The knowledge of N/m (Table I) allows a direct evaluation of the susceptibility effective mass. For

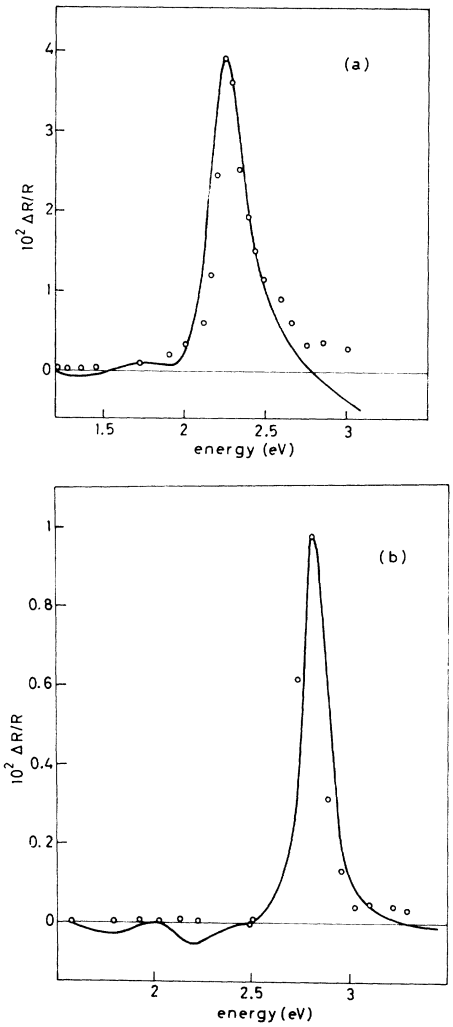

FIG. 5. Comparison between experimental electroreflectance spectra (solid line) and theoretical modulated reflectance, as derived from McIntyre-Aspnes model; $x = 0.52$ (a) and $x = 0.85$ (b). The adjustment of peak positions required energy shifts of -0.09 and $+0.03$ eV, respectively.

instance, one might assume that N equals the total number of valence electrons contributed by the sodium atoms, and calculate $m^* = N_{Na}(N/m)^{-1}$. Sodium concentrations are easily estimated following a known empirical relationship[5,23] which gives the lattice parameter as a function of stoichiometry; once this is done, one obtains for the effective mass of conduction electrons the set of values listed in Table II.

The figures so obtained are rather close to the value for a free electron, with a tendency to increase with increasing x. On the absolute scale, they are significantly lower than previous estimates from transport measurements,[9,10] and nearer to corresponding data for ReO_3,[10] or WO_3.[7] This would agree with currently accepted schemes of the electronic levels in ABO_3 compounds, tending to associate the properties of valence and lower conduction bands with the presence of the oxygen octahedra, regardless of the[10,12,24,25] A metal. In a rigid-band scheme different values of m^* should then indicate a different average curvature in those portions of the conduction bands that are swept by a Fermi level of increasing height. On the other hand the numerical values of m^* suggest that the overall shape of these bands is not far from parabolic. This conclusion appears to be reasonable, if one accepts that the conduction electrons be distributed over a set of states such as the t_{2g} manifold ($\Gamma_{25'}$, X_3, X_5) proposed by Mattheiss for ReO_3 or related compounds[25] (see for instance Fig. 6).

TABLE II. Values of sodium concentration and electronic effective mass for Na_xWO_3 of different stoichiometry; m_0 is the free-electron mass.

x	N_{Na} (cm^{-3})	m^*
0.52	0.927×10^{22}	$0.76\,m_0$
0.72	1.27×10^{22}	$1.02\,m_0$
0.85	1.49×10^{22}	$1.11\,m_0$

One can now turn to the other category of data reported here, i.e., electromodulated spectra and their connection to absolute spectra. The first and more pronounced structure is the A peak, appearing in the region of the plasma edge. As explained in Sec. III, its position and spectral shape are satisfactorily reproduced in terms of the McIntyre-Aspnes model, taking the dielectric data from direct ellipsometric measurements or related extrapolations. Large qualitative discrepancies were found when we attempted to fit the same spectrum to other models, such as a simple two-phase scheme resting on bulk modulation of the Na_xWO_3 substrate,[26,27] or the model of Cheyssac *et al.*[20] based on the modulation of surface conductivity. These facts certainly represent a good test for the model adopted and, at the same time, a proof of consistency for the optical data on which the evaluation was based.

Supposing that structure A is due to modulation of an interface layer, the question arises as to whether this layer is a modified phase of the metal substrate, or alternatively, of the electrolyte. At normal incidence, the two possibilities are not distinguishable from a mere fitting of the line shape.[22] In our analysis, however, figures were derived for the modulation factor $(\Delta N/N)d$, assum-

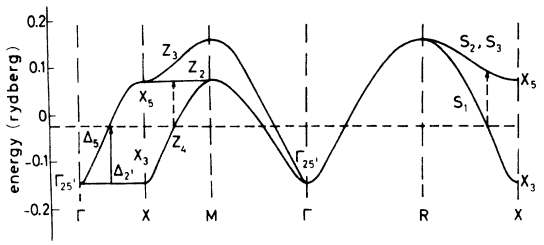

FIG. 6. Graphical representation of the lower conduction bands for ReO_3, as calculated by Mattheiss (Ref. 24).

ing the metallic case and matching peak values of $\Delta R/R$ to the pertinent expression, Eq. (6). If d is identified with the Thomas-Fermi screening length, one readily calculates $d \simeq 1$ Å (practically independent of stoichiometry). In combination with values of $(\Delta N/N)d$ quoted in Sec. III, one finds then $\Delta N/N = 85\%$; 50%; 11%, for $x = 0.52$; 0.72; 0.85, respectively. Such figures are not unreasonable, for applied fields in the order of 0.5×10^8 V/cm, as emphasized by other authors in similar cases.[20]

The above arguments give general support to the model which was assumed at the beginning for the A peak: namely, a structure arising from perturbation of the optical constants in a thin surface layer of the metal.

The marked decrease in modulation efficiency on going to higher electronic density might be difficult to explain, but is not in itself contradictory with our assignment. As a matter of fact, quantitative details are probably amenable to a particular shape of the potential drop across the metal-electrolyte interface, or to a more effective screening mechanism than the one postulated here.

Concerning the B structure we have already emphasized that it is not amenable to the same scheme and we accept the idea that it has little to do with screening effects.[28] An alternative interpretation may be attempted in terms of a band population effect, as proposed by Seraphin *et al.* for degenerate semiconductors.[26] The possible ambiguity as to which level (whether initial or final) is modulated, can be lifted considering the main features of this structure, in particular its shift to higher energy on passing from negative to positive polarization, or following the increase of stoichiometric ratio. Both indications, according to the quoted authors, give a strong support to the idea that the final level of the transition is at the Fermi energy.

A simple scheme would be the transition between a localized level and particular sets of empty conduction states around E_F. Indicating by E_0 the separation of this level from the bottom of the conduction bands, one writes for the transition energy

$$h\nu(x) = E_0 + E_F(x) . \tag{7}$$

Inserting the experimental values for $h\nu$, and substituting for E_F in terms of m^* and N_{Na}, this relationship gives values of E_0 that are negative and varying with stoichiometry. This apparent inconsistency cannot be lifted, unless arbitrary restrictions are made about effective masses or effective densities.

As an alternative, one can look for some kind of direct transition. Excluding transitions from valence bands to the Fermi level, which do not fit the magnitude of the observed energy, the remaining possibilities must be found within the lower manifold of conduction bands. They are illustrated in Fig. 6, with reference to the theoretical band scheme of ReO_3,[25] which we assume as a convenient basis of dicussion. The joint density of states evaluated for this scheme shows a small but significant peak between 1.5 and 2.0 eV, which matches the position of structure B (see Fig. 4). There are in principle three well-defined transitions compatible with this, as indicated by arrows in Fig. 6. However, only the transition $\Delta_{2'} \rightarrow \Delta_5$ fulfills the requirement of having its final state at the Fermi level, and therefore is the one matching the experimental evidence.

ACKNOWLEDGMENTS

The authors wish to thank Professor D. W. Lynch and Professor H. R. Shanks for kindly supplying the samples.

[1]P. G. Dickens, R. M. P. Quilliam, and M. S. Whittingham, Mater. Res. Bull. 3, 941 (1968); G. H. Taylor, J. Solid State Chem. 1, 359 (1969); S. Fujieda, Sci. Light 18, 1 (1969).
[2]F. Consadori and A. Stella, Nuovo Cimento Lett. 3, 600 (1970).
[3]G. Giuliani, A. Gustinetti, and A. Stella, Phys. Lett. A 38, 515 (1972).
[4]D. W. Lynch, R. Rosei, J. H. Weaver, and C. G. Olson, J. Solid State Chem. 8, 242 (1973).
[5]W. R. Gardner and G. C. Danielson, Phys. Rev. 93, 46 (1954).
[6]L. D. Ellerbeck, H. R. Shanks, P. H. Sidles, and G. C. Danielson, J. Chem. Phys. 35, 298 (1961).
[7]B. L. Crowder and M. J. Sienko, J. Chem. Phys. 38, 1576 (1963).
[8]L. D. Muhlestein and G. C. Danielson, Phys. Rev. 158, 825 (1967); 160, 562 (1967).

[9]H. R. Shanks, P. H. Sidles, and G. C. Danielson, Adv. Chem. 39, 237 (1963).
[10]J. Feinleib, W. J. Scouler, and A. Ferretti, Phys. Rev. 165, 765 (1968).
[11]S. K. Kurtz, International Meeting of Ferroelectricity, Prague, 1966 (unpublished), Vol. 1, p. 413; M. Cardona, Phys. Rev. 140, A651 (1965).
[12](a) M. Di Domenico, Jr. and S. H. Wemple. Phys. Rev. 166, 565 (1968); (b) M. Di Domenico, Jr. and S. H. Wemple, J. Appl. Phys. 40, 720 (1969).
[13]P. Camagni and A. Manara (unpublished).
[14]J. R. Beattie and G. K. T. Conn, Philos. Mag. 373, 222 (1955).
[15]J. R. Beattie, Philos. Mag. 373, 235 (1955).
[16]M. Born and E. Wolf, *Principles of Optics* (Pergamon, New York, 1964), Chap. 13.
[17]E. Landais, Bull. Soc. Fr. Mineral. Cristallogr. 91, 350 (1968).
[18]A corresponding anomaly is evident also in the ϵ_2 spectra. These effects might be due to the presence of impurities, defects, or to unknown layers formed at the surface of the samples, as a result of polishing treatments. No evidence of a reflectivity structure appears to have been found by other authors in this region.
[19]J. Feinleib, Phys. Rev. Lett. 16, 1200 (1966).
[20]P. Cheyssac, R. Garrigos, P. Kofman, L. Penavaire, J. Richard, and A. Saissy, Surf. Sci. 37, 683 (1973).
[21]T. E. Furtak and D. W. Lynch, Phys. Rev. Lett. 35, 960 (1975).
[22]J. D. E. McIntyre and D. E. Aspnes, Surf. Sci. 24, 417 (1971); J. D. E. McIntyre, *ibid.* 37, 658 (1973); J. D. E. McIntyre, in *Advances in Electrochemistry and Electrochemical Engineering*, edited by R. H. Muller (Wiley-Interscience, New York, 1973), Vol. 9, p. 61; J. D. E. McIntyre, *Optical Properties of Solids—New Developments*, edited by B. O. Seraphin (North-Holland, Amsterdam, 1976), p. 555.
[23]B. W. Brown and E. Banks, J. Am. Chem. Soc. 76, 963 (1954).
[24]A. H. Kahn and A. I. Leyendecker, Phys. Rev. A135, 1321 (1964).
[25]L. F. Mattheiss, Phys. Rev. 181, 987 (1969); Phys. Rev. B 6, 4718 (1972).
[26]R. Glosser and B. O. Seraphin, Phys. Rev. 187, 1021 (1969); R. Glosser, J. P. Fisher, and B. O. Seraphin, Phys. Rev. B 1, 1607 (1970).
[27]A. Prostak and W. N. Hansen, Phys. Rev. 160, 600 (1967); 174, 500 (1968).
[28]We tend to exclude the possibility that structure *B* is due to a surface plasmon as the observed values of ϵ_1 and ϵ_2 in this region do not seem to fulfill the appropriate conditions.